

# Radiolucent pressure sensors

For mammography applications

David Bondesson & Amitoj Deo

June, 2014



**LUND**  
UNIVERSITY

Master's Thesis

Faculty of Engineering, LTH

Department of Biomedical Engineering

Supervisors: Martin Bengtsson & Magnus Dustler

Skåne University Hospital, Malmö

## Abstract

In a mammography examination, an x-ray image is taken of the patient's breast. The examination can be painful due to the fact that the breast has to be properly compressed to attain good image quality. To reduce discomfort for the patient it has been suggested to measure pressure distribution over the entire breast.

This thesis investigates design and manufacturing of a radiolucent pressure sensor and its possibility to be used in mammography applications. The fabrication of the sensor, included a conducting polymer PEDT which was used to create a matrix system of sensors. This was the conducting layer that together with dielectric materials created a capacitive pressure sensor. Durability and calibration tests were also performed to determine application possibilities of the sensor.

The results showed that the manufactured pressure sensor was radiolucent. Thus, this invention could be implemented in a mammography machine without negatively affecting its screening process. Further research is needed to ensure that the sensor would act expectedly in a real breast compression test.

## Acknowledgements

This Master's thesis has been done at the Department of Biomedical Engineering at LTH and by close collaboration with the division of Medical Radiation Physics, SUS Malmö.

There are many people who have contributed to this project whom we would like to thank:

From the Department of Biomedical Engineering, LTH: Martin Bengtsson, Researcher, our main supervisor who contributed during all stages of this project and always had the time to help. Without his interest and knowledge this project would not have been completed. Mikael Evander, Researcher, for his help with the design and manufacturing of the electronic circuit board. Fredrik Ejserholm, Ph.D. student, who helped with equipment.

From the division of Medical Radiation Physics, SUS Malmö: Magnus Dustler, Ph.D. student, our supervisor who always was at hand and helped with tests and had many ideas. Pontus Timberg, Researcher, for help with ideas and information. Maria Christiansson, Researcher, for help with radiation tests.

From the division of Solid Mechanics, LTH: Zivorad Zivkovic, Technician, for ideas and help with the measurement equipment.

From LU Innovation System, Lund University: Fredrik Edman, Patent Advisor, for help with ideas and information.

# Contents

1	Introduction.....	7
2	Theory.....	8
2.1	Pressure.....	8
2.1.1	Young’s Modulus .....	9
2.2	X-ray.....	10
2.3	Sensing techniques.....	11
2.3.1	Resistive.....	11
2.3.2	Piezoresistive.....	11
2.3.3	Capacitive .....	12
2.4	Capacitance .....	12
2.4.1	Capacitor .....	12
2.4.2	Capacitors in series.....	13
2.4.3	Capacitors in parallel .....	14
2.5	Mammography .....	17
2.5.1	Structure and anatomy of breasts.....	17
2.5.2	Mammographic screening.....	18
2.5.3	Mammographic examination .....	18
2.5.4	MAMMOMAT inspiration.....	20
2.6	Photolithography.....	21
3	Method.....	23
3.1	Fabrication of sensor .....	23
3.1.1	PMMA layer.....	23
3.1.2	PEDT layer.....	23
3.1.3	PDMS layer .....	25
3.1.4	Polyimide layer .....	26
3.2	Completed sensor.....	28
3.3	Fabrication of multiple sensors .....	28
3.4	Calibration of sensors.....	30

3.5	Calibration while pressure over all sensor points .....	31
3.6	Transparency test .....	32
3.7	Durability tests of sensor.....	32
3.7.1	Radiation test .....	32
3.7.2	Thermal test .....	33
3.7.3	Compression test.....	34
3.8	Measurement .....	34
3.8.1	Retrieve signal .....	34
3.8.2	Process signal .....	36
4	Results .....	38
4.1	Transparency test .....	38
4.2	Calibration of sensors.....	40
4.2.1	PDMS thickness .....	40
4.2.2	Calibration of matrix sensor system.....	40
4.2.3	Calibration while pressure over all sensor points .....	41
4.3	Durability tests .....	42
4.3.1	Radiation test .....	42
4.3.2	Thermal test .....	43
4.3.3	Compression test.....	43
4.3.4	Retrieve and process signal.....	44
5	Discussion .....	45
5.1	Durability tests .....	45
5.2	Calibration of sensors.....	45
5.2.1	Calibration while pressure over all sensor points .....	46
5.3	PEDT difficulties.....	47
5.4	Development of polyimide layer .....	47
5.5	Conclusions.....	48
6	Suggestions for improvements.....	49
6.1	Laser-cutting of PEDT layer .....	49

6.2	Bonding technique .....	49
7	Bibliography.....	50
8	Appendix 2. Scientific article .....	53
8.1	Radiolucent pressure sensors - for mammography applications.....	53

# 1 Introduction

Mammography is a diagnostic method where x-ray radiation is used for locating tumors in breasts. In such an examination a breast is put under pressure and an x-ray image is taken. This is possible due to the fact that tumors appear brighter on the x-ray image, and can therefore be identified.

While the procedure is performed, the breast's compression is performed with two pressure plates. Compression is done to limit radiation dosage and improve image quality. The method has been shown to be uncomfortable and painful, since pressure is applied until the patient considers it to hurt. Unfortunately, it can therefore scare the patient and cause distress. Not much has been researched regarding the pressure applied over the breast but it is assumed that the more a breast is compressed the better image can be created.

Studies have investigated possibilities to lessen the pressure applied on the breast by turning focus to the necessity of high pressure [1]. By adding focus to how pressure is applied over all parts of the breast, it opens up ways for optimization.

Such a method has previously been suggested in a Master Thesis done by M.Dustler and P.Fröjd at LTH ("Pressure distribution over breasts during mammography") Issues arise however due to the sensor being visible in the mammography screening and actually disturbs the examination.

Thus the idea to create radiolucent pressure sensors arose. The benefit of these would be that the sensor would not have to be removed after measuring pressure, thus assuring that imaging will be performed over the same area and while the breast is compressed exactly the same.

In this project several 3x3 radiolucent pressure sensors have been created as prototypes and tests performed to show their possibility to be implemented with mammography screening. A capacitive pressure sensor was chosen due to its advantages in sensitivity and from lack of disturbances by temperature changes.

To add an economical and environmental aspect to the project, durability is also taken into consideration through testing. Tests were performed to see how often the sensors are in need of recalibration and if they can withstand regular exposure levels of radiation, would it be implemented in an actual screening machine. Design and how sensors are manufactured of such a pressure sensor are investigated in this project. An electronic system is additionally presented which reads out the data acquired by the sensor matrix.

Considering that radiolucent pressure sensors are a new invention, the sensors and their application are currently being patented [2]. The patent is applied for in parallel with a system in which the sensor matrix could be implemented [3].

## 2 Theory

### 2.1 Pressure

Pressure is defined as the force applied, divided by the area that the force act on, which can be seen in Eq. 1 and figure 1.

$$P = \frac{F}{A} \left[ \frac{N}{m^2} \right] \quad (1)$$

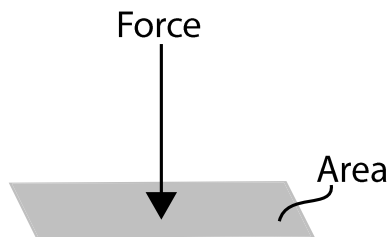


*Figure 1. An overview of pressure, which is force divided by the area that the force is applied on. The grey part in the figure is the part that the force is applied to.*

Pressure has the unit Pascal. It is important to identify what pressure is actually being measured, since a sensor is affected by the atmospheric pressure (101.3 kPa) at rest. This is used as the “zero-level” pressure in many systems. This is a reason why it’s very important to know if a pressure is measured relative to another pressure or to vacuum.

Pressure measured from gases or liquids are different compared to pressure exerted mechanically (with a force, onto an object). The pressure from an object is only divided on the surface that is in direct contact. In conclusion, the pressure from an object in contact with another object will mostly not be uniformly distributed over the surface, if the surfaces are not entirely flat, see figure 2. To expand on this one can add that even objects that appear to be flat have surfaces that are very likely uneven, which is why the pressure is not distributed uniformly [4, p. 5] .



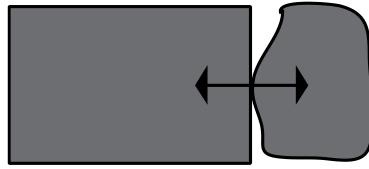


Figure 2. Two objects in contact with each other. The right object is not entirely flat resulting in that the pressure is only distributed on the contact area. The arrows indicate the direction of the force that each object “feels”.

### 2.1.1 Young’s Modulus

When a force is applied on a solid object, the shape of the object tends to change. It can for example stretch, compress or shear. When the force applied on the object is removed and the object does not return to its original shape, it means that the object has been deformed. However if the object do return to its original shape it is called elastic. Most objects are elastic up to a certain limit, and will after that start to deform.

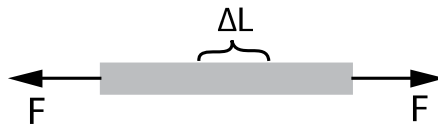


Figure 3. The length of a solid bar is increased as it is subjected to forces according to the picture. The increased length of the solid bar (due to the forces) is shown as  $\Delta L$ .

In figure 3, a solid bar can be seen. Two forces are acting on it causing the length of the bar to increase. The increase in length is shown as  $\Delta L$  in the figure. Strain is defined as the change in length divided by the initial length of for example a solid bar, see Eq. 2.

$$\text{Strain} = \frac{\Delta L}{L} \quad (2)$$

Stress is another important property that can be calculated, and is defined as the ratio between the force and the cross sectional area, see Eq. 3.

$$\text{Stress} = \frac{F}{A} \quad (3)$$

In figure 4, the stress vs. strain curve can be seen for a solid bar. Until point A the stress is proportional to the strain. The ratio between the stress and the strain in this region is called Young's modulus, see Eq. 4.

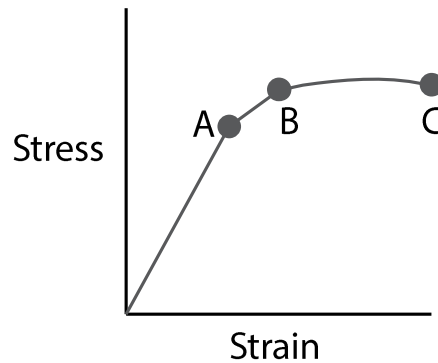


Figure 4. A stress vs. strain graph. Until point A, which is known as the proportional limit, the strain is proportional to the stress. After point B (the elastic limit) the object will be deformed. Point C is known as the fracture point, after this point the object will fracture.

$$Young's\ Modulus = \frac{Stress}{Strain} = \frac{F/A}{\Delta L/L} \quad (4)$$

Young's modulus is often used to characterize materials. A material with a high Young's modulus is not flexible, whereas a material with a low Young's modulus is elastic. Examples are: diamond (Young's modulus: 1220 GPa), rubber (Young's modulus: 0.01-0.1 GPa) [5].

## 2.2 X-ray

Imaging of the body by the use of x-rays is very common today in hospitals. Radiation that is used is electromagnetic and has much higher frequency than visible light. Most x-rays lies in the energy range 100 eV to 100 keV. The radiation used in these applications is created in a device called x-ray tube, which consists of a glass cylinder with vacuum. In this cylinder there is an anode and cathode working as electrical poles. When voltage is applied between the anode and cathode, electrons are accelerated from the cathode, and collide with the anode. As an electron come closer to the atomic nuclei, it starts to feel the electric field from the nuclei, thus its speed decreases and a change occurs for the electrons trajectory. As this happens, the electron loses some of its energy, which will be sent out as x-rays (see figure 5).

In mammography screening radiation hits the patient, and some of it will penetrate everything without any effort, some of the photons will on the other hand lose all the energy in the body and not be able to penetrate through to hit the detector screen. Some of the radiation will interact in the patient's body and change direction, and will not be useful to the image contrast. That kind of radiation is removed by a kind of filter before it reaches the film.

The fact that bones in the body have higher atomic number than some other tissues concludes that some photons will stop at the bones. An x-ray image basically shows how dense some areas of the body are. The white parts of the image are areas where the photons have been attenuated more than the black parts of the image [6].

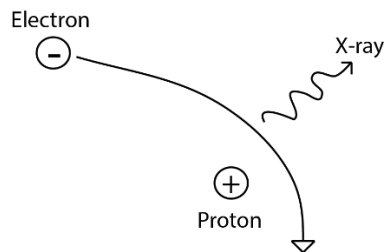


*Figure 5. As the electron comes close to the proton, its trajectory changes, which results in loss of energy that is sent out as x-rays.*

## 2.3 Sensing techniques

The basic idea of a sensor is to respond to a physical input, and give a correlated output signal. In this project the input signal is pressure. When it comes to tactile sensors, there are three different techniques used to measure a pressure, described below. For this project the capacitive sensing technique is used.

### 2.3.1 Resistive

When a conducting material is physically deformed it changes its conductance. This can be used to measure pressure by knowing the change in resistance. A sensor of this kind is called a resistive sensor. The main problem with this method however is its low sensitivity. Its main advantage is a linear correlation between pressure and output signal.

### 2.3.2 Piezoresistive

A piezoresistive sensor will measure the resistance caused by a deformation of the material. Piezoresistivity is a property of a material that describes the material's ability to deform, when a voltage is applied over the material. A reason to use this kind of sensors is that in a piezoresistive material the change in resistance at a specific pressure, is much greater than for other materials. However, piezoresistive materials are sensitive to specific temperatures and some of these

materials are also sensitive to light as an input. This is the case for silicon [4, p. 6].

### 2.3.3 Capacitive

A capacitive sensor measures the capacitance between two electrodes. Since a capacitive sensor is not affected by temperature changes along with the fact that it has high sensitivity, this is the sensing mechanism that will be used to measure pressure in this project. Issue might arise however when trying to distinguish how to extract the signal. Capacitance is also inversely correlated with frequency which therefore has to be stable. Another problem is that when measuring capacitance the actual signal is reactance which is a combination of the resistive and the capacitive load.

## 2.4 Capacitance

Capacitance is a measure of the ability of a capacitor to store electrical charge, and is described as the ratio between charge and voltage ( $C = Q/V$ ). Capacitance has the unit farad (coulomb/volts).

### 2.4.1 Capacitor

Capacitors have been used widely since they were discovered and are applied in following situations:

- To filter signals
- To transform voltage
- To store energy (backup capacitor)

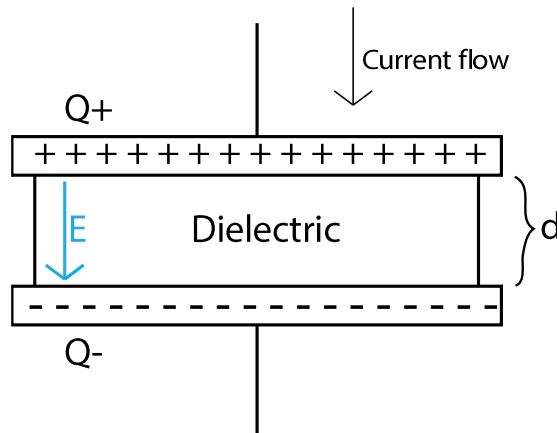


Figure 6. Overview of a capacitor.

As can be seen in figure 6, a capacitor consists of two conductors separated by a distance  $d$ . The conductors are usually metallic. Between the two plates another material, the dielectric is situated.

If a current moves from top to bottom as illustrated, it means that electrons will move from bottom to top. While the electrons are moving up they gather on the lower plate of the capacitor. The result of this is that the lower plate will be negatively charged, which in turn will produce an electric field in the dielectric (the direction of the field is shown by the blue arrow). The electric field will force the electrons to leave the upper plate at the same rate that they gather on the lower plate. The result of this is that current appears to flow through the capacitor [7, p. 92].

The voltage across the capacitor is a measure of the amount of energy stored in the capacitor. The net charge over the capacitor is always zero, since one of the conductors holds the charge  $Q+$  and the other one holds  $Q-$ . The capacitance over a parallel plate capacitor is calculated by the use of Eq. 5.

$$C = \frac{\epsilon A}{d} \quad (5)$$

Where  $d$  is the distance between the two conducting materials,  $A$  is the area of each plate and  $\epsilon$  is the dielectric constant for vacuum ( $\epsilon = 8.85 * 10^{-12} F / m$ ) [7, p. 99]. According to the equation for the capacitance above, a smaller distance between the plates will lead to a higher value of the capacitance.

It's also possible to calculate the energy stored in the capacitor with Eq. 6.

$$E = \frac{1}{2} CV^2(t) \quad (6)$$

Where  $C$  is capacitance, and  $V$  is voltage between the plates [7, p. 96].

#### 2.4.2 Capacitors in series

When capacitors are connected in series like in figure 7, the total amount of capacitance measured can be calculated by Eq. 7.

$$\frac{1}{C_{tot}} = \frac{1}{C_1} + \frac{1}{C_2} + \frac{1}{C_3} + \dots + \frac{1}{C_n} \quad (7)$$

Where n is the number of capacitors.

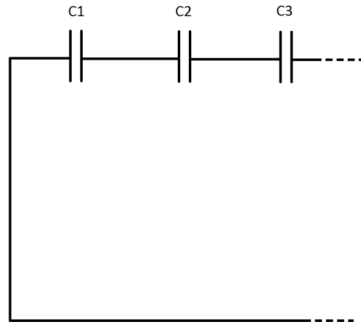


Figure 7. Schematics of serially connected capacitors

### 2.4.3 Capacitors in parallel

When capacitors are connected in parallel like figure 8, the total amount of capacitance measured can be calculated with Eq. 8.

$$C_{tot} = C_1 + C_2 + C_3 + \dots + C_n \quad (8)$$

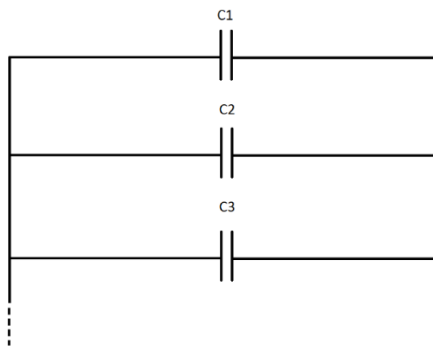


Figure 8. Schematics of capacitors connected in parallel

## Dielectric

The material between the two conducting plates is called dielectric. Dielectric materials act as insulators, which means that the electrical charges cannot move freely. There are three main reasons for why a dielectric is put between the conducting plates in a capacitor:

- To make sure that the conducting plates do not come into contact with each other. This makes it easier to have a smaller plate separation, which in turn leads to higher capacitance.
- The dielectric reduces the strength of the electric field, which leads to a higher capacitance.
- It reduces possibility of dielectric breakdown, which is the dielectric starting to act as a conductor, when a high voltage is applied over it.

As stated before, charges in a dielectric material cannot move freely, this does not on the other hand mean that they can't move at all. When a dielectric material is put in an electric field the positive sides of the nuclei will move with the field and the electrons will move against the field (see figure 9). Electric field lines start on positive charges and finish on negative charges. Through figure 9, it is observable that the field lines in every stressed atom or molecule in the dielectric material actually point in the direction opposite to the external electric field. This results in a reduction of the total electrical field between the two conducting plates. This result helps a lot, since the decreased electric field leads to the possibility for the capacitor to hold the same amount of charge at a lower voltage. In other words the output capacitance is increased, since it is inversely proportional to  $E$ , where  $E$  is the electric field [8].

When a dielectric is put into an electric field it is said to be polarized, the polarization can occur in two alternative ways: rotation and stretching. This however is a subject that will not be elaborated upon more in this thesis.

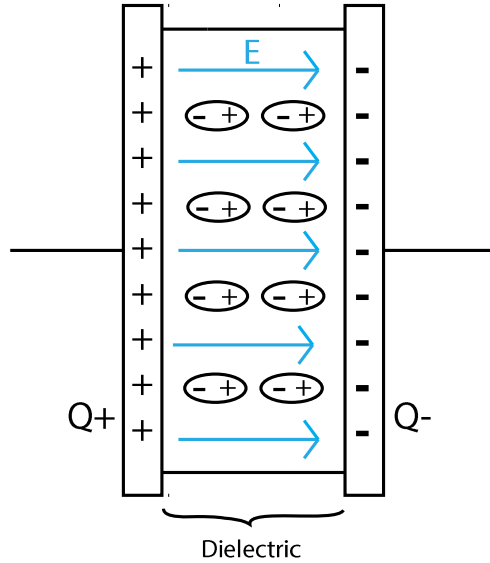


Figure 9. Polarization of the dielectric, resulting in a smaller overall electric field, and a higher capacitance for the capacitor. Which is the basic reason on why to put dielectric materials between the conducting plates in a capacitor.

The dielectric constant (also known as the relative permittivity)  $\epsilon_r$  is a dimensionless value. To measure this for a given dielectric the following principle is used, which is performed under static electric fields. Firstly the capacitance is measured between the plates of a given capacitor (vacuum between the plates) which will provide a value  $C_{vacuum}$ . While keeping the distance between the conducting plates constant, the dielectric is now put into the capacitor, and a new capacitance is measured,  $C_{dielectric}$ . All dielectric materials have  $\epsilon_r > 1$ . To obtain the dielectric constant the formula below is used (Eq. 9).

$$\epsilon_r = \frac{C_{dielectric}}{C_{vacuum}} \quad (9)$$



In table 1 below a number of dielectric materials can be seen along with their dielectric constants [9].

Material	Dielectric constant( $\epsilon_r$ )
Air	1.00059
Paper	3.7
Glass	4-6
Water	80
PDMS	2.3-2.8
Durimide	3.2-3.3

Table 1. Dielectric constants for different materials.

## 2.5 Mammography

### 2.5.1 Structure and anatomy of breasts

The size and exact structural composition of the female breast varies widely from person to person. The breast consists mostly of fatty and connective tissue, which can be described as “soft tissue”. Also included in the term “soft tissue” is glandular tissue which takes care of milk production. This consists of lobules and vessels connected towards the nipple area. Despite the areola having a set place behind and around the nipple, its propagation also varies widely from subject to subject. With this difference in propagation, density of the areola also varies.

During the female aging process the glandular tissue will be replaced with fatty tissue which appears as a change in both structure and density [4].

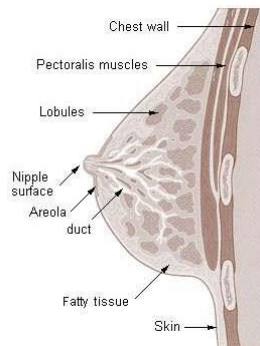


Figure 10. Schematic of breast [10]

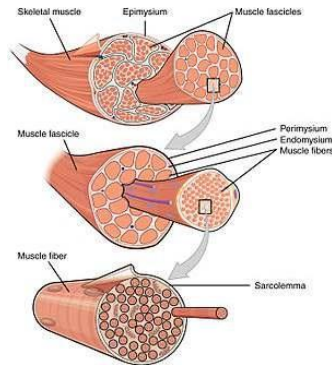


Figure 11. Muscle fibers [11]

From figure 10, the breast can be seen to cover the pectoral muscle. The muscle has what should be noted from that is the muscle's mechanical properties, which differ from those of the breasts'. This is because it consists of muscle fibers which can be seen in figure 11. The muscle's mechanical properties also differs greatly from person to person.

### 2.5.2 Mammographic screening

During the mammography screening, x-ray radiation is used to create an image of the breast. Because a tumor has higher x-ray absorption than fatty breast tissue, cancers can be detected. The screening is thus used to detect tumors at an early stage. For this reason its diagnostic capability are performed on cases of suspected sickness or periodically in standard screening of asymptomatic women. In cases where potential tumors are found, the patient is further examined to strengthen diagnosis.

It is the peculiar growth pattern of malignant tumors that allows this detection, as both connective- and glandular tissue absorbs x-rays largely identically to cancerous tissue. For this reason, trained radiologists are required to evaluate mammograms. This method can show abnormalities before the cancer grows enough to become palpable and thus noticeable to the woman.

### 2.5.3 Mammographic examination

A mammographic examination consists of several stages. Firstly, the breast is compressed by a pressure plate controlled by the operator. This is done for the following reasons:

- The thinner the breast, the shorter is the distance that x-rays need to travel through it. A shorter distance means less x-rays are absorbed and also that they do not scatter as much, reducing both the dose to the patient and the noise in the image.

- By compressing the breast, the different structures are spread out and separated reducing the problem of overlapping tissue.
- When imaging is performed it is very important to keep the breast still to avoid motion blur. For this reasons, pressure plates will hold the breast in the same place throughout the scanning.

The operator will carefully increase force between pressure plates until the breast is compressed enough. The set force usually varies with the mechanical properties of every patient [12]. The maximal value of the machine is 200 N which is almost twice as high as usually required. Even if the breast is properly compressed it will be harder to diagnose a breast with higher density [13].

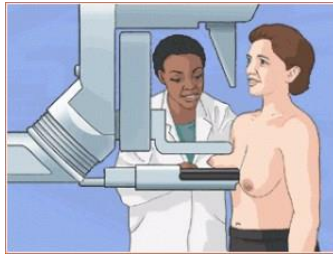


*Figure 12. Ongoing mammography screening [14]*

Two images per breast are taken and if suspicious abnormalities that could be interpreted as tumors are found, the patient will be called back where she/he is requested to participate in more screenings and tissue samples to confirm or refute the diagnosis. Ultrasound and MR imaging can also be performed for assurance.

The images in a regular mammography screening will be taken from above (craniocaudal CC) from head to foot and from the side (medolateraloblique MLO). Figure 13 and 14 shows two examples from such images that are later used to create a 2-dimensional image. In the 3-dimensional case a tomosynthesis is performed which photographs the breast in a specified range of angles to build the full model.

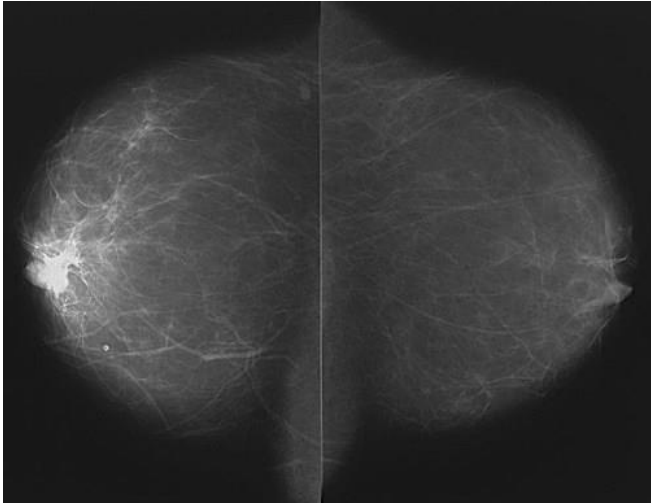


*Figure 13. Screening image of breasts bilateral craniocaudal CC [15].*

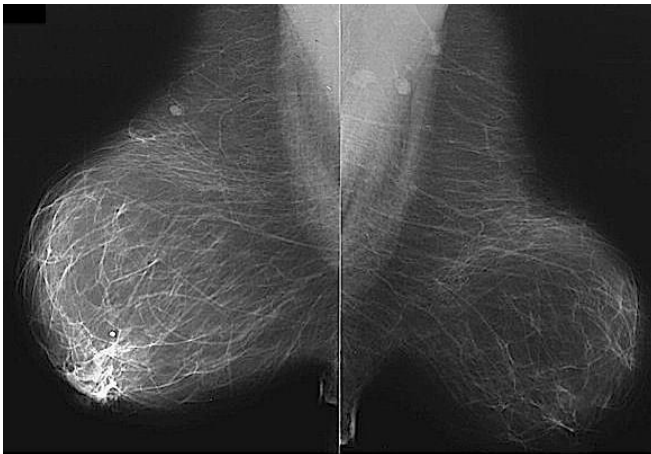


*Figure 14. Screening image of breasts bilateral medolateraloblique MLO [15].*

#### 2.5.4 MAMMOMAT inspiration

The machine used in this project for testing sensors was MAMMOMAT inspiration (Siemens AG, Erlangen, Germany) that can be used for regular mammography screening. The imaging steps consists of positioning the breast on the table as seen in figure 12. A compression plate is afterwards lowered manually until desired position and compression is acquired. The plate has three speed settings. Before the breast is reached, the compression is performed quickly until resistance is met. Next the compression velocity is lowered partly for the patients comfort and partly for a possibility to optimize compression.

Optimization can for instance be performed through specific settings in the machine that compares compression to applied force and stops when added force does not result in sufficient reduction of thickness. The current force over the compression plate is measured with  $\pm 5$  N accuracy. A display shows the distance between table and plate, which in this situation translates to breast thickness.

Several compression plates of different sizes are available. Flexibility differ between the plates to have more options for patients in case of great discomfort. Attention is necessary however to observe the effects of differences in pressure distribution around breast when using different plates [4].

MAMMOMAT inspiration operates between 23-35 kV, where V in this case refers to tube voltage. In case of regular setting of 25 kV and maximum power the machine have a possible range between 2-560 mAs depending on setting [16]. Lower values of voltage could be used to enhance contrast but only for thinner breast. Determination of correct radiation dosage is calculated inside the machine based on several important criteria.

## 2.6 Photolithography

The process of creating patterns in e.g. a polyimide by the use of UV-light is known as photolithography. A photoresist is built up by three constituents, which are: a polymer (the structural properties of the resist), a photoactive compound (this part is a light sensitive compound, sensitive to a narrow band of UV-light), and a solvent [17, p. 69]. Photolithography is a widely used technique to pattern materials, especially in microelectronic systems. In figure 15, the method to pattern these materials can be seen. The photoresist is firstly spun on to for example a wafer, or another kind of material in the construction. After that it is exposed to UV-light, depending on if the photoresist is negative or positive, some of the parts of the photoresist will be removed in the developing process.

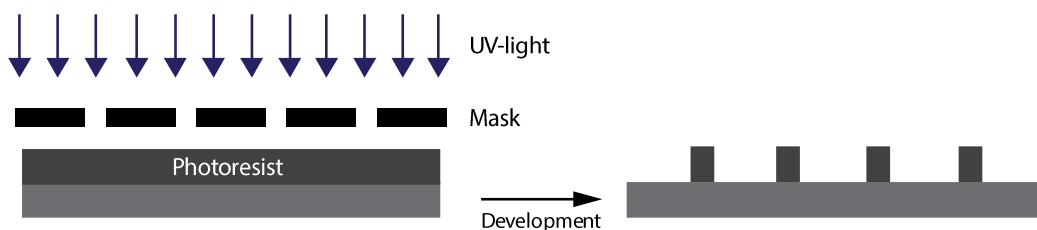


Figure 15. The process of photolithography. A mask is put onto the photoresist. The design of the mask will decide the structure of the upcoming photoresist. The photoresist in this figure is negative, meaning that the exposed parts will disappear after the development process.

If a positive resist is used and exposed to UV-light, the exposed parts will become soluble after the development process, meaning they will disappear. The opposite effect is observed if a negative resist is used, the unexposed parts disappears after the development process.

## 3 Method

### 3.1 Fabrication of sensor

The fabrication of the sensor consists of several layers on top of each other. Two parts were made separately and then attached to each other. The complete sensor consists of 6 layers (see figure 16), the process to create each layer is described below.

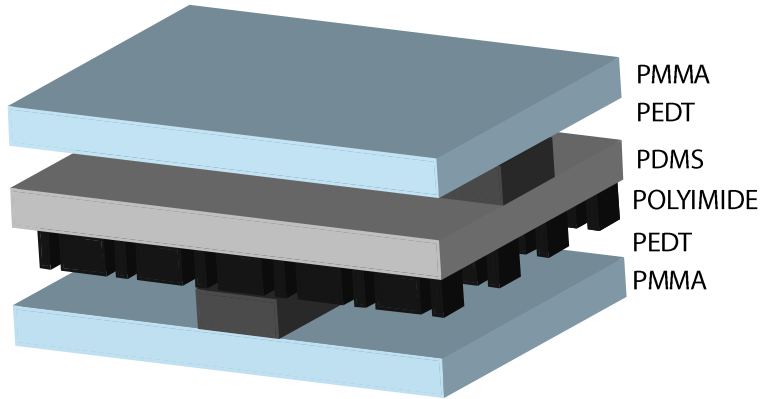


Figure 16. The final sensor with all the layers implemented. The three top layers as well as the three bottom layers were made separately. The two parts were attached to each other in the end.

#### 3.1.1 PMMA layer

Polymethyl methacrylate (PMMA) is a transparent and stiff plastic. PMMA is often used as a substitute for glass, since it has the highest surface hardness of all thermoplastics. It has high light transmission and a high resistance to UV-light [18]. The top and bottom layers of the sensor (see figure 16), are both PMMA. The bottom layer is thicker (2 mm). The upper layer has a thickness of 250  $\mu\text{m}$ .

#### 3.1.2 PEDT layer

Poly(3,4-ethylenedioxythiophene) (PEDT) is a polymer which is very robust and highly conductive. This polymer can be coated onto several materials, by either spin-coating or printing techniques. PEDT was originally developed for antistatic coatings [19].

To create a PEDT layer, a technique called spin-coating was used, which is a technique to add thin films on to flat substrates. This technique was also used when creating the PDMS and polyimide layers. When creating polymers this method is the most common. The process started by adding the liquid PEDT to the middle of the substrate (in this case the PMMA layer). The substrate was then rotated at high speeds causing the PEDT material to be spread over the substrate

by the centrifugal forces. By adjusting the spinning velocity the desired thickness of the layer was achieved. Spin coating was then completed by placing the substrate in an oven to remove the solvents, see figure 17.

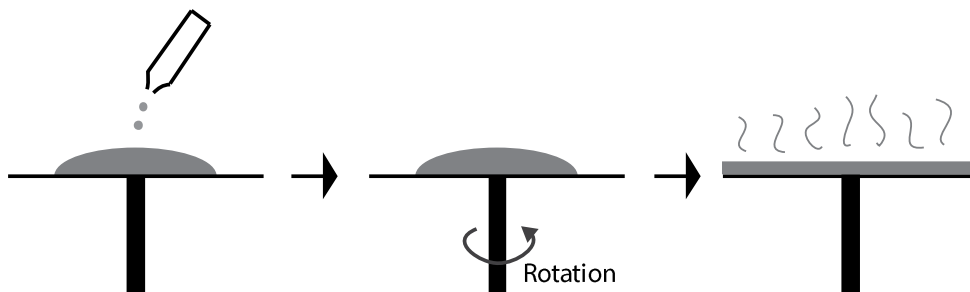
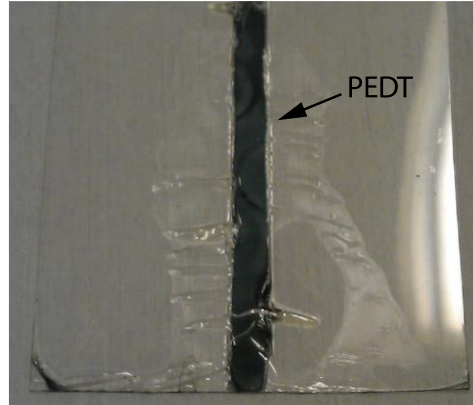


Figure 17. Overview of spin coating. The process is started by adding the PEDT (in this case) to the substrate. By spinning the substrate the desired thickness of the film can be accomplished. The procedure is finalized by "baking the substrate" to remove the solvent.

The polymerization solution was made through a mixture created in two steps. Firstly 3.9 g Fe(III)tosylate was mixed with 5.85 g butanol which is a weight ratio of 1:1.5 in favor of butanol. This was then shaken until the two compounds were fully solved. Secondly 2 ml of butanol was mixed with 0.15 ml pyridine and 0.22 ml of EDT. This was also shaken and the two mixtures were combined.

PMMA was covered with PVC- plastic, 70  $\mu\text{m}$  thick, to get a rectangle with a thickness of about 0.5 cm. 1.5 ml PEDT was first put on the PMMA, and the spinning process was started. After the spinning was completed, the whole part was put in an oven at a temperature of 60°C for 5 minutes. The PEDT layer (still with the tape attached) was then cleaned with a mixture of anisol and butanol (50% of each). The spinning was completed with two speeds: 1: 250 rpm for 10 seconds, 2: 500 rpm for 30 seconds. This procedure corresponds to a PEDT thickness of 6  $\mu\text{m}$ .





*Figure 18. Production of PEDT on top of a PMMA plastic layer. Image shows the result after the removal of the tape.*

As it can be seen in figure 18, the PEDT is spun on to both the plastic PMMA and the thicker PMMA located at the bottom, both the procedures are the same.

### 3.1.3 PDMS layer

Polydimethylsiloxane (PDMS) is a type of silicone rubber that has many applications. PDMS is very elastic and has unique flexibility properties. The elasticity is characterized by Young's modulus  $E$ , which is the stress applied on the material divided by the strain (describes the relative change in shape and size of materials while a pressure is applied) along the same axis. The Young's modulus for PDMS varies between 1-100 MPa. PDMS is also hyper elastic which means that young's modulus is not constant, but decreases as it is stretched. The Poisson ratio of PDMS is 0.5, which means that if the material is elongated by 20%, the material will become 10% thinner. The softness of this material has the advantage that it will not damage other materials that are in contact with the PDMS.

It is biocompatible (it is even commonly used for breast implants) due to its relatively inert characteristics. The material will expand when heated because it has a high thermal expansion coefficient. The effect of this is that smaller patterns will become sensitive when the temperature starts to rise. It is however still usable in a temperature range from  $-100^{\circ}\text{C}$  to  $100^{\circ}\text{C}$  [20, pp. 22-24].

This material was highly interesting in this application since it was placed between the two conducting PEDT layers as one of the two dielectric materials. The dielectric constant for PDMS is 2.3-2.8 [21]. A higher value is better when used as a dielectric in a capacitor, resulting in a higher capacitance. Higher in this context relates to air where the dielectric constant is around 1.

Before the spinning of the PDMS layer was started, tape was attached to the split up the PEDT where the cable was attached. The mixture of PDMS consisted of two parts: 10 ml silicon oil and 1 ml of curing agent (the ratio of silicon oil to curing agent is 10:1). The spinning of the PDMS was done by adding 3 ml of PDMS to the PMMA and PEDT layer, placing the plate on the spinner and start it. The velocity was set to 850 rpm (for 60 s) which corresponded to a thickness of 100  $\mu\text{m}$ . It was then put into an oven at a temperature of 60°C for about 30 minutes and was left to rest for 24 hours until the procedure was continued.

Sensors were made with three different thicknesses of the PDMS layer (50, 75 and 100  $\mu\text{m}$ ). To achieve a thickness of 100  $\mu\text{m}$ , the spinning was done with a speed of 1000 rpm (for 60s). 50  $\mu\text{m}$  thickness was attained with a speed of 1560 rpm (for 60 s).

### 3.1.4 Polyimide layer

Durimide 7520, a negative photoresist, is the polyimide of choice in this project. The benefits of this material is that it has excellent adhesion. The range of thicknesses for this material varies between 2-50  $\mu\text{m}$ . Young’s modulus is 2.5 GPa. Like the PDMS layer, The Polyimide layer between the conducting PEDT layers is acting as a dielectric. The dielectric constant of this polyimide is 3.2-3.3 [22]. Polyimide is a negative photoresist. This means that the parts that are exposed to UV-light will become insoluble when they are in contact with the photoresist developer, see figure 19.

For this layer, only Durimide 7520 was used. The aim was to achieve a thickness of 25  $\mu\text{m}$  for the polyimide layer. The same spin-coating method was used to properly distribute the polyimide over the sensor plate. Spin velocity was set to 1800 rpm for 1 minute (2ml was used) which are values taken from previous studies [22]. After that it was put in the oven for 20 minutes at a temperature of 80°C.

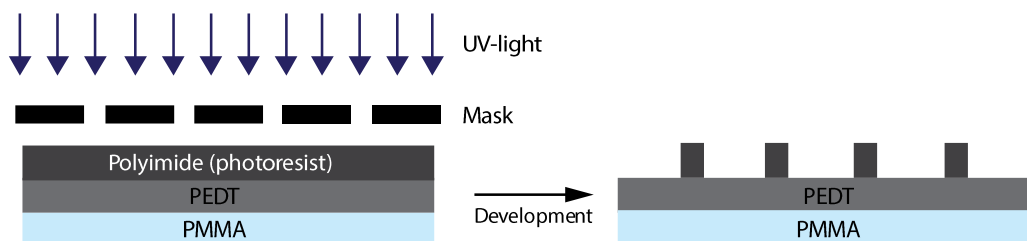
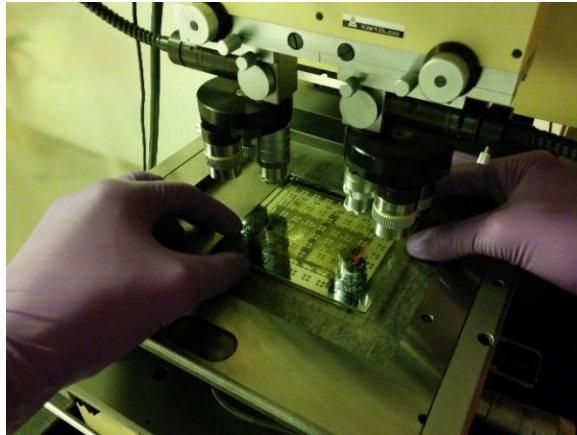


Figure 19. Photolithography, where the result is a change of character of the polyimide layer. After that the photoresist layer has undergone the UV-light process, it is developed with the use of HTR-D2 and RER600 (removes the waste). The desired structure is then acquired.

To remove some parts in this layer, UV-light was used (see figure 20 and figure 21) together with a mask to attain the desired arrangement of the layer. During this process it was important to align the mask and photoresist carefully so that the pattern will correspond to the desired design. The functionality of the mask was to allow light to shed on only some areas (see figure 19).

The thickness of the polyimide layer was measured to be 15-20  $\mu\text{m}$  with an optical measurement method, involving a microscope. The system included a sensor that measured the height of the microscope table, where the layer that we wanted to measure was located on. By focusing on the edge and on the layer beneath, the height of the layer could be found.



*Figure 20. The process of alignment of the sensor and the mask before the UV-light exposure.*

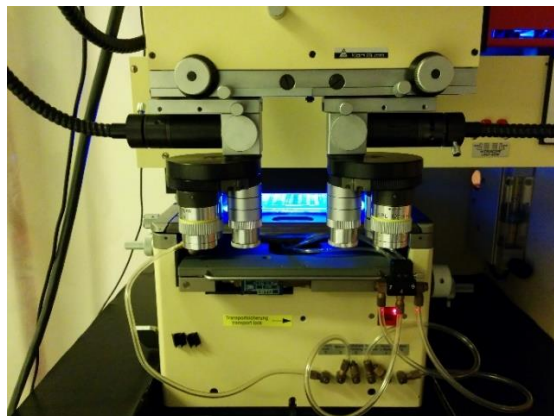


*Figure 21. The sensor is under exposure.*

The layers were allowed to rest for 24 hours before the development process was started. That process was done by using HTR-D2 for two minutes and then RER-600 for 1 minute to remove the waste on the polyimide layer. After the

completion of the developing process the layers were put in an oven (80°C) for 1 minute to further harden the resist.

### 3.2 Completed sensor

The two layers, were then attached to each other so that the PEDT on each layer were cross-aligned. The top layer containing the PMMA film was put slightly off center on the lower layer. This was done to simplify the process of attaching cables to the sensor. The sensor is shown in figure 22, where the overlap of the two layers can be seen. The cables were attached to the sensor with conductive epoxy glue.

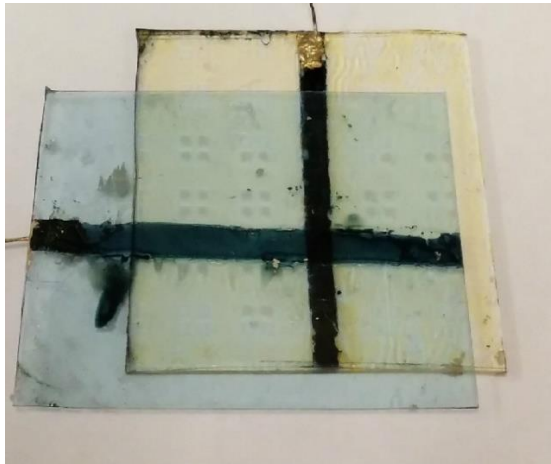


*Figure 22. The sensor with attached cables. The two layers are placed with a displacement over each other to make room for the cables to be attached to the PEDT material.*

### 3.3 Fabrication of multiple sensors

In the construction of multiple sensors, the idea was to have three stripes of PEDT material on both the plastic film and the thicker PMMA. With the two layers put on top of each other crosswise, the result was a 3x3 sensor system, with a total of 9 sensors. The thicker and thinner PMMA used in the fabrication was cut to 6x6 cm. Before the spinning of the PEDT material took place, the PMMA and the plastic film was covered with PVC-tape on those areas where the PEDT was not supposed to attach. The same procedure was used to spin the PEDT on the layers.

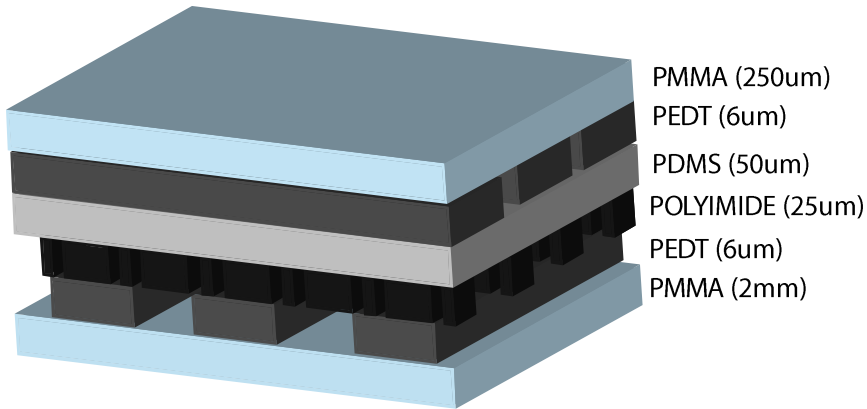


Figure 23. Three PEDT stripes are constructed on top of the PMMA and the Plexiglas film. The width of the PEDT layer is 0.5 cm and they are separated by a distance of 1 cm. The thickness for each layer can also be seen.

The spinning of the PDMS was made as before, where the aim was to achieve a thickness of 50  $\mu\text{m}$ . A different mask was used when the Polyimide layer was exposed to UV-light. The reason for this was that the holes that were created in this process were going to be placed more tightly together. This makes the pressure not being distributed over a bigger surface when the PDMS is pushed together. The results of more holes in the polyimide layer will lead to more space for the PDMS to be squeezed into. The benefit of this was that when pressure was applied on the sensor, the PDMS was not pushed to the sides, affecting the values of other pressure points.

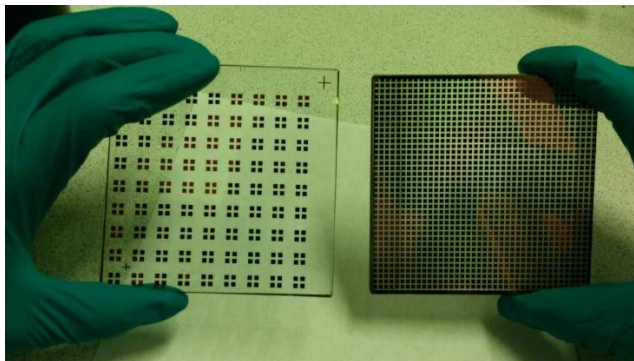


Figure 24. The masks that were used during the UV-light exposure of the polyimide layer. The mask to the left is the old one used in the previous design when fabricating only one sensor. The mask to the right is used in the new design.

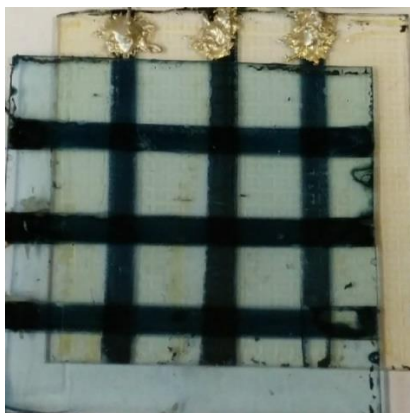


Figure 25. A prototype of a sensor array. Each crossing between the PEDT layers consists of one sensor, meaning that the total sensors is 9 on this 6x6 cm area.

### 3.4 Calibration of sensors

In order to calibrate the sensor a LCR-meter from HP was used (4262A Hewlett Packard). This device generates a test signal of 1V. The frequency of this signal can be chosen from three values: 120 Hz, 1 kHz, and 10 kHz. The measurements were performed using the 1 kHz signal.

The calibration was done by placing known weights on top of the intersection of the two PEDT layers and at the same time reading out the capacitance displayed on the LCR-meter (see figure 26).



Figure 26. Calibration of the sensor, by placing known weights and reading out the capacitance on the LCR-meter.

The following weights were used to calibrate (gram): 0, 2, 5, 10, 20, 50, 100, 200 and 500. A circular shaped plastic part was placed on the crossing of the two PEDT layers and the weights were put on top of that.

The actual thickness of the PDMS layer depends on the spin speed and also on the duration of the spinning. The speeds for the different thicknesses were taken from [23]. For confirmation of these values an optical method was used to attain the focal point, to find out the thickness.

The following thicknesses was found for the corresponding PDMS layers (table 2).

Assumed PDMS thickness ( $\mu\text{m}$ )	Measured thickness ( $\mu\text{m}$ )
50	$60 \pm 5$
75	$85 \pm 10$
100	120

Table 2. Measurement of the real thickness of the PDMS layers.

### 3.5 Calibration while pressure over all sensor points

A more realistic test for the sensor would be to put pressure over all nine pressure points at once, and see the reaction and reliability of the sensor. A 3 mm thick plexiglas board was put on the sensor, covering all points. 3 points were calibrated with this method, point 1, 5 and 9. Since the layers are not equally thick at all points on the sensor, these three points were chosen because they are situated across the sensor, see figure 27.

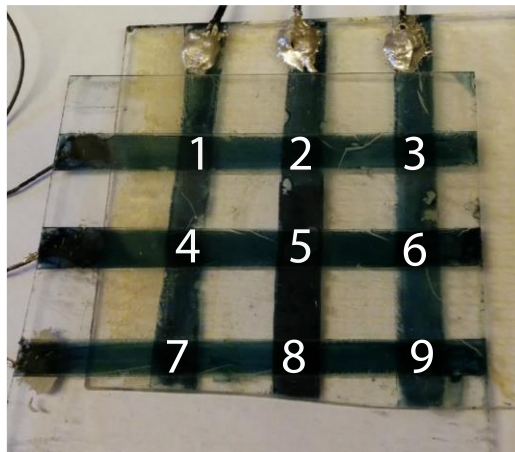


Figure 27. Each sensor point is associated with a number.



### 3.6 Transparency test

To test if the conducting parts of the sensor would be detectable on an x-ray image, an x-ray transparency test was done. This was done by using the mammography machine, Siemens inspiration. The test was done at SUS Malmö. In figure 28 the setup can be seen. The sensor was placed on a thicker PMMA plastic part. When the x-ray image was taken, there was no pressure on the sensor. The image was taken with screening energy set to 28 kV at 56 mAs, which is equivalent to a regular breast screening.



*Figure 28. Siemens MAMMOMAT machine taking an x-ray image of the sensor. The white arrow shows the sensor.*

The resulting picture was afterwards analyzed in Matlab through its image processing toolbox. With this, statistical information was extracted from the circumscribed areas in figure 34 to figure 37 seen below. The mean value and standard deviation of pixel values in the images, converted to grayscale images, were the basis of analysis.

### 3.7 Durability tests of sensor

Three tests were performed to test the sensors durability properties, a radiation test, a thermal test and a compression test.

#### 3.7.1 Radiation test

This test shows the sensors ability to perform after having been irradiated as it is meant to be in regular usage of mammography screening. The test was done using an x-ray machine by Siemens, Gammatron 3 (see figure 29). This machine is both



older and stronger than today's mammography screeners, but will show if the sensors are absorbing radiation and deteriorate from usage. The x-ray machine was originally used during the end of the 1970s and its radiation source is Cobalt-60 ( $^{60}\text{Co}$ ).



Figure 29. The Gammatron 3, used for radiation tests.

To get an idea of the amount of radiation that the Gammatron 3 was capable of, the radiation was measured before the actual test of the sensor. After a test for 2 minutes, the value 243 mSv was given, by the radiation source (Co-60). During a screening, 4 exposures per patient are used. This means a total of 8 mGy for each patient (with the use of the reference value 2 mGy per exposure). The radiation source can only be used continuously for 20 minutes. By letting the sensor to be exposed  $4 * 20$  minutes, we get around 10000 mGy, which gives:  $10000/8 \text{ mGy} = 1250$  patients. Since a machine at Malmö hospital takes around 300 patients per week, the radiation that the sensor is exposed to corresponds to 4 weeks of usage.

### 3.7.2 Thermal test

This test simulates long time usage of the sensor. The increased thermal exposure simulates a fastened aging process which results in wear and tear on the polymer layers [24]. The method consisted of measuring values for a single sensor, after putting the same sensor in an oven for 1 week at the temperature of  $40^{\circ}\text{C}$ . When the test was finished a final measurement was performed.

As a side note, material was found that suggest that the PDMS layer will expand in a heated environment [20, p. 24]. Considering however that the PDMS was created in  $60^{\circ}\text{C}$  and also retracts to its previous form, it shouldn't become a problem since test measurement is performed long after it has cooled.

### 3.7.3 Compression test

This test evaluates the effects of long time deformation on the sensor to help estimate life expectancy. The idea is to place a 500 g weight on the sensor, and let it stay there for 1 week. The test should show the ability of the materials to withdraw to its initial form.

This is important not only for the PDMS layer, but for the other layers as well. The risk is that a deformation may occur and increase the capacitance, thus creating the need to recalibrate sensors more often. Before starting the second measurement the sensor was left without weight for 1 hour after the 500 g weight was removed to make sure only permanent changes were tracked.

## 3.8 Measurement

To extract a good signal, a measurement of capacitance compensating for several error sources is needed. To perform such a measurement, proper tools are vital for distinguishing what is resistive load and what is capacitive. A great deal of effort is also invested in processing the retrieved signal which, in its final stage, should be useful for building a medical image of the density distribution of the measured tissue. For these reasons, the retrieval of the signal is divided into two parts, software and hardware/software. The software includes a Matlab script written to handle information that is sent in on a computer port where the hardware is connected.

### 3.8.1 Retrieve signal

The hardware/software part makes sure that the signal is read and sends (via integrated software) information to a device that translates an SDA (Serial Data Line) signal to a digital signal. The software part then keeps track of retrieved information and builds an image based on the pressure distribution via a GUI.

Figure 30 shows a schedule of the hardware/software scheme that visualize the idea of how to obtain a signal from the pressure matrix.

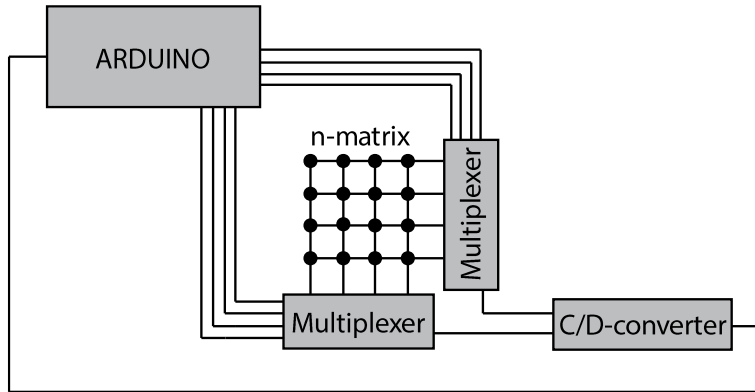


Figure 30: schematic of measurement system hardware part.

It also shows the pressure matrix being wired to two multiplexers. These determine a port from which to retrieve the capacitance signal. The signal is read with the capacitance-to-digital converter, which converts the analog capacitance signal to an SDA. These parts are the building blocks of the hardware/software part and are controlled by an Arduino Leonardo unit. The Arduino is described as an open source electronics prototyping platform [25] and is used in this project as a bridge between hardware and software, due to its ability to convert signals between both.

The Matlab program tells the whole circuit how and when new measurements should be performed. For simplification, a complete GUI was made in Matlab to

- Connect Arduino with Matlab.
- Choose ports on Arduino to communicate with.
- Perform measurement over the whole matrix to create the final image.

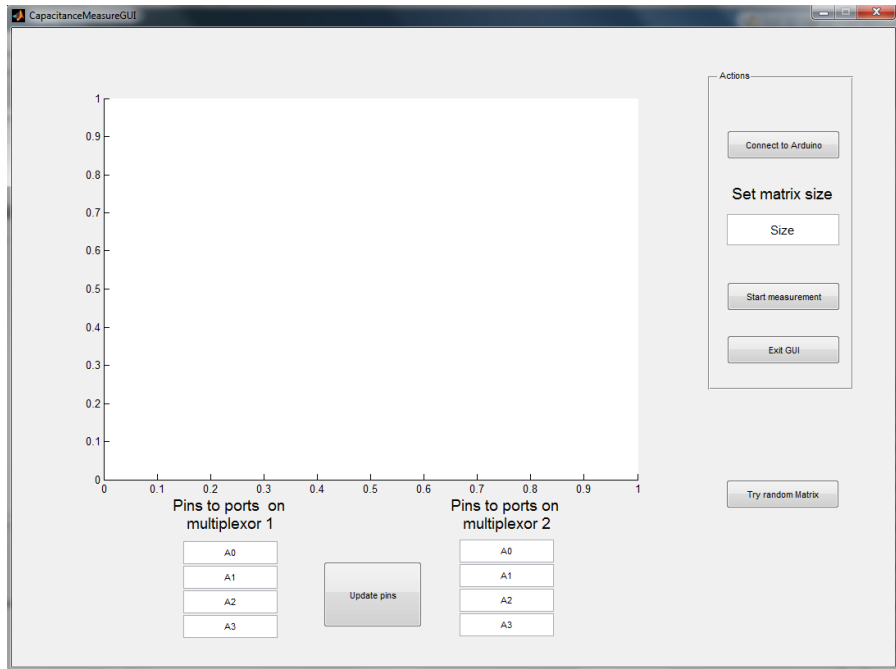


Figure 31. Matlab GUI setup. The program first requires a connection with an Arduino device to perform any operation. After a connection is established it will wait for specific pins on the Arduino to be set as integers. The standard values A0-A3 represent ports on the multiplexers, which aid in remembering which pin goes to which port. Measurement is then performed by pressing the “start measurement” button and the values are plotted 3-dimensionally with Matlab’s surf function.

For simplification of the Matlab code, an interface written with Arduino code called “I2C block for ArduinoIO simulink package” [26] was used. This interface was obtained from Mathworks homepage where users have the possibility to share their own code. It implements functions from Arduino programming into Matlab so that the code could be written similarly in Matlab as in Arduino

### 3.8.2 Process signal

While extracting the signal from the multiplexors it is important to notice that given value will not only come from the required point in the sensor, e.g. port 1 on both of the multiplexors will not retrieve the exact signal on the top left sensor in the 3x3 matrix. Instead what is measured is a combined capacitance from the whole matrix system which can be seen as several capacitors connected in series and parallel. Figure 32 shows the above mentioned example where capacitance is measured in the top left corner. In it the other sensor point’s capacitance will be added in parallel with the required signal and thus increase the complexity of retrieving it.

All measurement will give their own combination of the different capacitances between the two connections, thus giving a system of linear equations. To solve

this system, sufficient measurements need to be performed to calculate the actual values of every point. This is where the multiplexers become the obvious choice for connecting with the matrix. They can retrieve a signal in  $n^2$  different ways which is exactly the amount of unknown variables that we have. We therefore have a solvable matrix system.

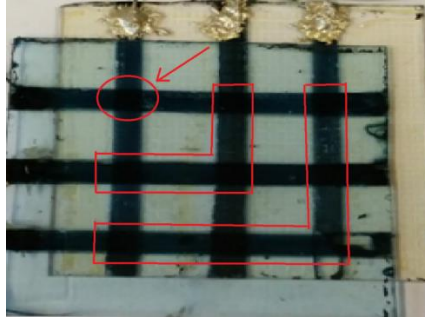


*Figure 32. Visualization of how different sensor points are connected. Desired pressure point is connected in parallel with the other two parts which will be the total capacitance measured.*

## 4 Results

### 4.1 Transparency test

The radiolucency is an important property of the sensor. This was tested by taking an image of the sensor with the use of a machine made by Siemens (Mammomat Inspiration). In figure 33 the image of the sensor can be seen. The sensor is placed over a bigger plastic part, the cables and the conductive epoxy that is used to attach the cables can easily be seen, this will be solved by making a bigger sensor and taking out the signal at a larger distance from the image area. The PEDT material cannot be seen at all in the image. Evaluation from Matlab's image processing toolbox show no significant changes in statistical properties that would support a noticeable change.

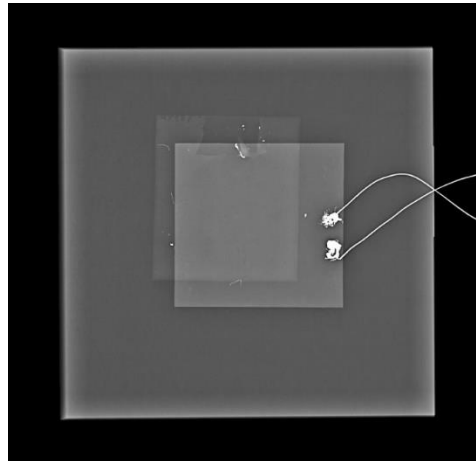


Figure 33. X-ray image taken of the sensor at Malmö hospital with the use of Mammomat Inspiration, Siemens. The PEDT material in the sensor is not seen at all in the image.

	Mean	Standard deviation
PEDT1	119.04	3.95
PEDT2	118.31	2.99
No PEDT 1	118.75	3.84
No PEDT 2	119.10	3.61

Table 3. Statistical characteristics of specific regions from figure 33. Measurement show the average pixel values and standard deviation in specified regions. Regions are shown in figure 34 to figure 37.

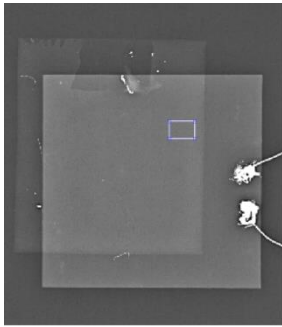


Figure 34. Second Image without any PEDT in stressed area. In table called no PEDT 1

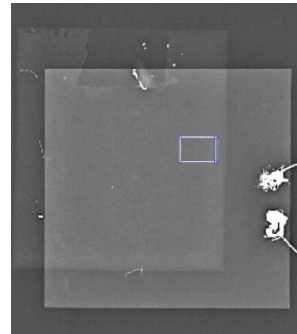


Figure 35. Second Image without any PEDT in stressed area. In table called no PEDT 2

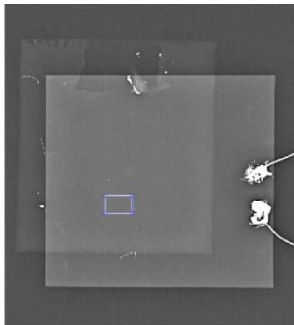


Figure 36. Image with PEDT both halves of sensors. In table called PEDT1

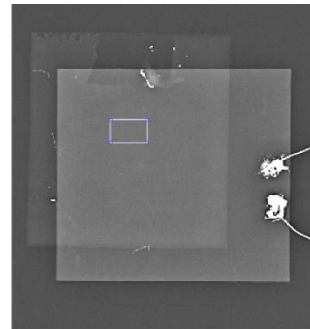


Figure 37. Image with PEDT on one half of sensors. In table called PEDT2

## 4.2 Calibration of sensors

### 4.2.1 PDMS thickness

In figure 38 the output capacitance for a given pressure (in kPa) can be seen. The measurement was performed for different thicknesses of the PDMS layer. Three sensors with different PDMS thicknesses were created.

The sensor with 50  $\mu\text{m}$  thickness had the widest range (6.6 pF to 17.1 pF) in capacitance and was also the one that seemed to have the best resolution among the three. This thickness was chosen for the PDMS layer.

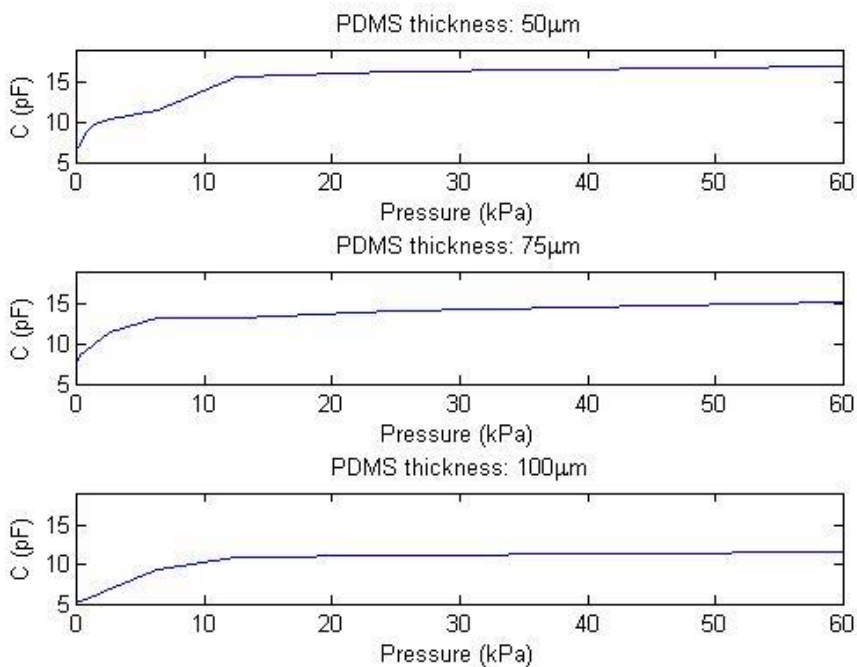


Figure 38. Three sensors with different PDMS thickness (50, 75 and 100  $\mu\text{m}$ ) were calibrated. The capacitance can be seen for applied pressure on each sensor.

### 4.2.2 Calibration of matrix sensor system

The result after calibrating a matrix sensor can be seen in table 3, all 9 points were calibrated, which can be seen in figure 27.



	1	2	3	4	5	6	7	8	9
Pressure (kPa)	pF	pF	pF	pF	pF	pF	pF	pF	pF
0	5.1	7.2	7.1	5.5	9.7	8.1	4.2	7.2	7.1
0.2	5.7	8.5	7.7	5.6	10.3	8.5	4.5	8.0	8.1
0.6	6.2	9.7	8.3	6.0	10.9	9.0	4.9	9.2	9.1
1.2	6.8	11.8	9.6	6.3	12.0	9.6	5.3	10.7	10.3
2.5	7.3	14.3	11.6	7.0	13.2	10.6	6.0	12.9	11.1
6.2	7.7	15.5	13.2	7.5	14.7	12.2	7.3	15.1	12.3
12.5	8.3	15.7	15.0	7.8	5.4	13.5	7.7	15.9	12.9
24.5	8.4	16.0	16.9	8.0	16.1	13.9	7.9	16.6	13.9
62.5	8.5	17.2	17.5	8.3	16.8	14.9	8.2	17.5	14.2

Table 4. Capacitance values for all 9 pressure points on the sensor.

#### 4.2.3 Calibration while pressure over all sensor points

The results for this test can be seen in the figures below. In figure 39, the three pressure points were calibrated as earlier, by placing pressure only at the corresponding point. In figure 40, the pressure was applied over all 9 pressure points, and the three chosen points were calibrated again.

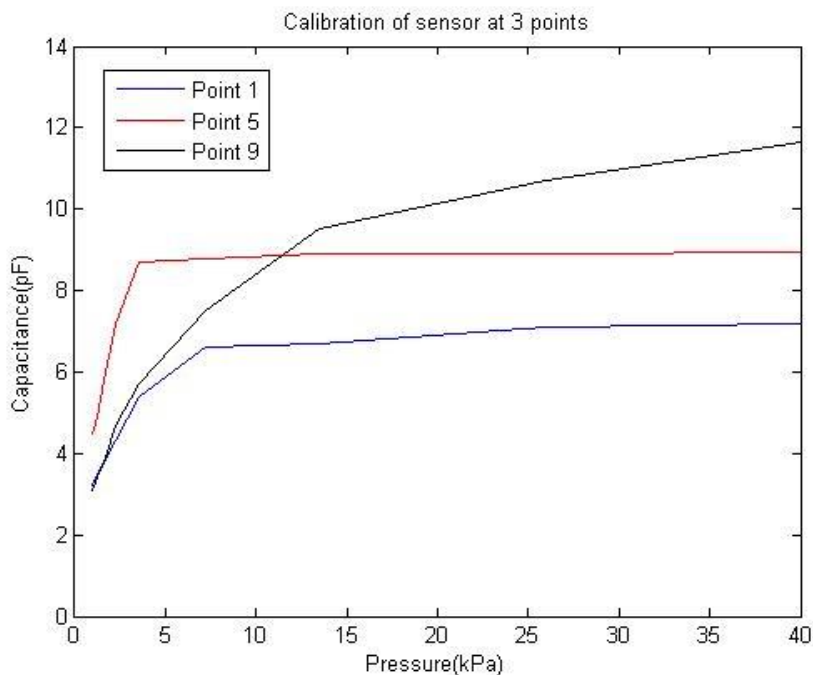


Figure 39. The three points were calibrated by applying pressure on each point. See figure 27 to see the exact location of each point.

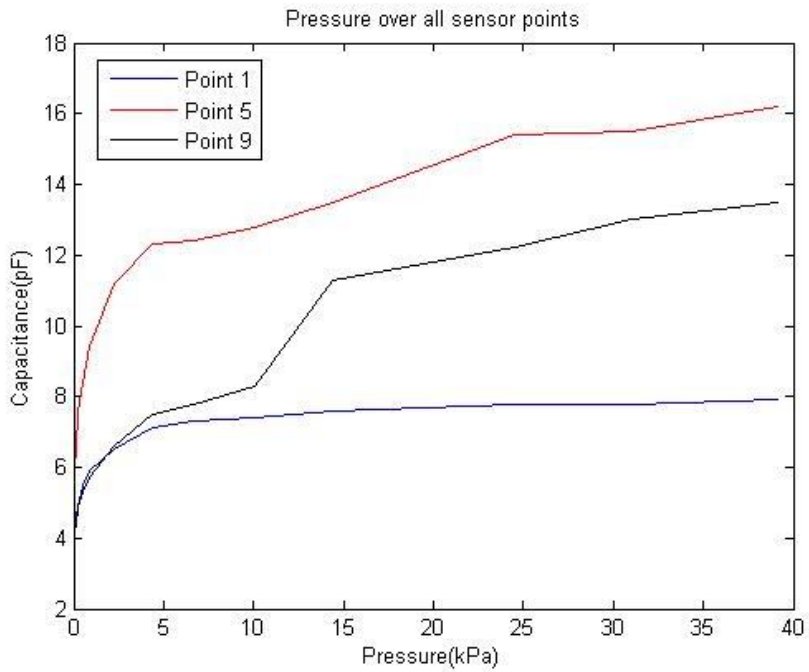


Figure 40. Same three points were calibrated, this time the pressure was applied over all sensor points at the same time.

### 4.3 Durability tests

#### 4.3.1 Radiation test

Pressure (kPa)	Capacitance before (pF)	Capacitance after (pF)
0	4.4	4.3
0.2	4.4	4.4
0.6	4.5	4.5
1.2	4.6	4.6
2.5	4.8	4.8
6.2	5.6	5.4
12.5	6.4	6.3

24.5	7.2	7.0
62.5	7.5	7.3

Table 5. Capacitance measurements before and after the radiation test of the sensor.

The capacitance measurements were done before and after the radiation test. Table 5 shows the result. As can be seen very small changes occur that can hardly be considered to correlate with the performed test.

#### 4.3.2 Thermal test

Pressure (kPa)	Capacitance before (pF)	Capacitance after (pF)
0	2.9	2.9
0.2	3.0	3.3
0.6	3.2	3.5
1.2	3.5	3.6
2.5	3.8	3.9
6.2	4.4	4.4
12.5	5.3	5.3
24.5	5.8	6.0
62.5	6.4	6.5

Table 6. The measured capacitance before and after the heat test. The measurement of the capacitance after the test was done 1 hour after the completion of the test.

In table 6 the results of the thermal test can be seen.

#### 4.3.3 Compression test

Pressure (kPa)	Capacitance before (pF)	Capacitance after (pF)
----------------	-------------------------	------------------------

0	2.7	3.3
0.2	2.8	3.4
0.6	2.9	3.6
1.2	3.2	3.9
2.5	3.6	4.1
6.2	4.4	4.8
12.5	5.0	5.6
24.5	5.7	5.9
62.5	6.2	6.5

*Table 7. The difference between the capacitance, before and after the compression test. The measurement of the capacitance after the test was done 1 hour after the removal of the weight.*

The measured curve for given pressures remains similar after the deformation. Before this test was performed, the sensor was calibrated, and the capacitance for a 500 g applied weight was 6.2 pF. After 1 week of continuous pressure from this weight, the observed capacitance had increased to 7.1 pF showing that a deformation actually occurs in the PDMS.

#### 4.3.4 Retrieve and process signal

The electrical circuit manage to transfer the capacitance signal through the multiplexers. However when attempting transmission between the capacitance converter and the Arduino, short circuit appears continuously.

## 5 Discussion

### 5.1 Durability tests

The durability tests give an indication of the potential sustainability of the finished product. The radiation test showed that the sensors will work without absorbing too much radiation. Noted though, that the energy from a mammography machine is usually around 30keV, while the radiation source used (Co-60) emits at 1.17 MeV or 1.33 MeV. Higher energy means more penetration, but the damage should not be more than twice on the sensor. More tests should be conducted where the sensors are irradiated while measuring to tell if they will function while a mammography screening is running. The reason for not getting the exactly the same values from the sensor is likely related to that the applied weight needs to be positioned in the same place to replicate exact values.

The purpose of the thermal test showed that a simulation of wear and tear over time will not negatively affect the sensor's properties and thus it might be possible to create sensors that will last for an extended period of time. This is important in a sustainability aspect, both environmentally and financially where the first has an ever increasing importance when developing new material for future use.

The compression test shows that a deformity has occurred which was supported from the increased capacitance before taking off the weight. The increase showed that a high amount of strain over an extensive period of time can affect future values correlated to the extent of the deformation. It should be noted that these changes occurred after a week of constant and high pressure. This is a lot more intense testing than what will occur during treatment. The result also shows that even after this rough treatment, one hour of resting is enough to return to a very similar curve type. Therefore it can be concluded that although the sensor has deformed a little, all that is needed is recalibration.

### 5.2 Calibration of sensors

Measurements were attempted with all three frequencies, however at low frequencies (120 Hz) there were too many fluctuations for the displayed values on the device, low resolution was also observed when using this test signal. The same phenomena was observed when the frequency of the test signal was set to 10 kHz. The most stable output from the LCR-meter was observed when a test signal with the frequency 1 kHz was used, fluctuations of  $\pm 0.1$  pF were seen.

To attain as good values as possible from the sensor the idea is to create several sensors with different thickness of the PDMS layer. The initial sensor that was fabricated has a PDMS thickness of 100  $\mu\text{m}$  and a capacitance between the values 5.3 pF and 11.9 pF was attained with zero and maximum pressure. An idea is to

increase the thickness of the PDMS layer to get better resolution, however a larger distance between the conducting PEDT layers will lead to a lower capacitance.

### 5.2.1 Calibration while pressure over all sensor points

From point 1 and point 9 in figure 39 and 40, it can be noted that they share similar output capacitance. When instead pressure is applied over the whole sensor, an increase of total measured capacitance on the same points can be noted. This supports previously discussed theory that the surrounding sensors add extra capacitances to selected node. Point 5 which is located in the center of all pressure points, does not show the same characteristics. A possibility for this is a disturbance in PEDT pattern which can be seen in figure 41. There seems to be something wrong with the thicknesses of the corresponding layers at exactly this point. However, results from the first two points show that it is possible to create sensors that has all pressure points working accordingly.



*Figure 41. The middle PEDT pattern is not uniform, the arrow shows a part of the layer which consists of no PEDT at all.*

### 5.3 PEDT difficulties

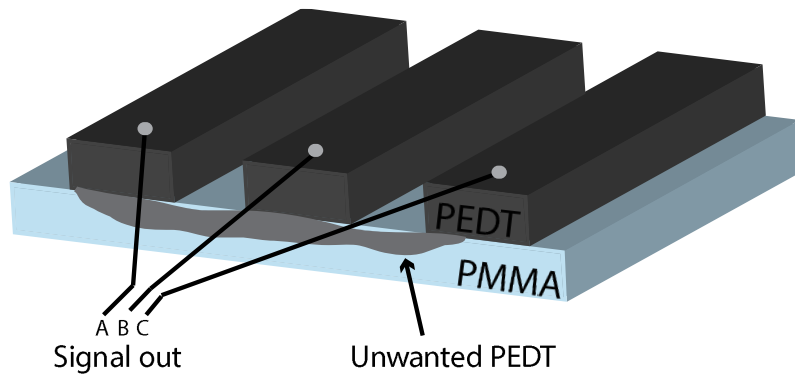


*Figure 42. After the spinning of the PEDT layer, some of the PEDT attached on the sides of the PMMA layer, which caused problems.*

When measurements were done with a completed sensor, it was observed that the measured capacitance signal was much greater than preliminary calculations had revealed. After the spinning of the PEDT layer, it was observed that some PEDT had stuck on to the sides of the PMMA layer and needed to be removed. By looking at figure 42, one can observe that the extra PEDT on the sides leads to an issue. This is that when the signal is measured for the left PEDT layer (signal A), the signals from B and C are also added, since the PEDT on the sides connects all the three layers. This can be solved by attaching tape on the side of the PMMA layer as well when fabricating the layer.

Another issue that was found with PEDT was that after the spinning process, the layers sometimes cracked at some parts. The reason for the cracking material is related to how high voltage the material can withstand. Cracks also occurred when the PEDT was baked in an oven because it contracted slightly on the PMMA plate when the temperature increased.

### 5.4 Development of polyimide layer

The development of the polyimide layer consists of putting the layer in solvents, when this was done for too long (sometimes 2 minutes for the HTRD2 solvent), the layer started to detach from the PEDT and PMMA layer. The reason for this is that the solvent starts to get under the polyimide layer and remove it that way. However timing is crucial, and continuous observation of the polyimide layers reaction to the solvent is needed to be able to respond as quickly as possible when small parts of the polyimide layer starts to detach.

## 5.5 Conclusions

Based on the results from the sections about radiolucency and calibration of both individual sensors and a matrix system it is possible to create a system that can measure applied pressure and at the same time be invisible in the electromagnetic spectra. More research is required in the topic of artefacts, specifically if the circuit is in need of protection from surrounding capacitive sources. These include the human body which can work as a capacitive load when it is in contact with the circuit. Evidence of such an artefact has been observed while measurements were performed and body parts came close to the sensors.

There is also room for discussion on how to properly calibrate sensors since no functional matrix was actually installed with the mammography machine. Many differences in results depends on position of the two parts when fabricating the sensors which showed when the two sometimes changed during measurement. It was however possible to reach similar values if the sensors were readjusted back to the original position and thus strengthen the idea of a system which gives consistent values when applying identical amount of pressure. To eliminate this error source in the durability tests the sensors were made sure to keep in exactly the same position between measurements.

The sensors worked well between 0-40 kPa though it should be noted that it is important with accurate measurements above 10-12 kPa since the change in capacitance decreases. Although, compared to mammography screening which is estimated to vary between 0-35 kPa, the sensors show promising results for being implemented in such a machine. In consideration of the capacitance curves for individual sensors with different thickness displaying possibilities to still notice change in ranges up to 60 kPa, it could be possible to use the pressure sensors in more than just mammography screening. More research should be performed in the area of optimizing sensor thickness for needed ranges.



## 6 Suggestions for improvements

### 6.1 Laser-cutting of PEDT layer

In order to create a matrix pattern of the PEDT layer, PVC tape was used. The thickness of this tape is an issue, and causes difficulties to cover the PMMA with PEDT. Another problem with tape is that it starts to get very tricky when matrix sizes bigger than 3x3 are needed, as the tape is attached manually. A better approach for the PEDT layer would be to cut the PEDT with laser. This would lead to straighter patterns and also bigger matrix systems would not be a problem to create with lasers.

### 6.2 Bonding technique

As described in the method of fabricating the sensor, two parts were made separately and then put together to form the sensor. The bottom layer consists of PMMA, PEDT and polyimide. The upper layer consists of PDMS, PEDT and PMMA. When these two layers are put together they stay attached for around 36 hours, and then the adhesion is no longer effective. A suggestion to solve this is to encapsulate the complete sensor to make it stay connected in the same place. Also to enhance adhesion an UV ozone cleaner used. The idea is to let the PDMS layer be exposed to ozone. This process removes molecular levels of contamination and might have a positive effect to make the two layers stick to each other.

## 7 Bibliography

- [1] M. Dustler, I. Andersson, D. Förnvik and A. Tingberg, "The effect of breast positioning on breast compression in mammography: a pressure distribution perspective," *SPIE journal of medical imaging*, vol. 8313, 2012.
- [2] M. Bengtsson, M. Dustler, A. Deo and D. Bondesson, "Functionally radiolucent pressure sensors". Patent Swedish Application 1400273-7.
- [3] Patent : international patent application PCT/EP2014/057372.
- [4] M. Dustler and P. Fröjd, "Pressure distribution over breasts during mammography," Lund University, LUND, 2010.
- [5] G. M. Paul A. Tipler, *Physics for scientists and engineers*, New York: W.H. Freeman and Company, 2008.
- [6] B. Jacobson, *Jacobsons Medicin och teknik*, Studentlitteratur, 2006.
- [7] A. R. Hambley, *Electrical Engineering, principles and applications*, Singapore: Pearson Prentice Hall, 2008.
- [8] G. Elert, "The Physics Hypertextbook," [Online]. Available: <http://physics.info/dielectrics/>. [Accessed 02 02 2014].
- [9] J. D. Jackson, *Classical Electrodynamics*, New York: Wiley, 1998.
- [10] "SEER Training Modules," 15 02 2014. [Online]. Available: <http://training.seer.cancer.gov/breast/anatomy/>.
- [11] "Open Stax CNX," [Online]. Available: <http://cnx.org/content/col11496/1.6/>. [Accessed 18 05 2014].
- [12] "IAEA," 20 02 2014. [Online]. Available: [https://rpop.iaea.org/rpop/rpop/content/informationfor/healthprofessionals/1\\_radiology/mammography/mammography-technique.htm](https://rpop.iaea.org/rpop/rpop/content/informationfor/healthprofessionals/1_radiology/mammography/mammography-technique.htm).
- [13] J. R. Dullum, E. C. Lewis and J. A. Mayer, "Rates and Correlates of Discomfort Associated with Mammography," *Radiology*, vol. 214, pp. 547-

552, 2000.

- [14] "Archive for mammography test," 17 02 2014. [Online]. Available: <http://onlinehealthcareservices.wordpress.com/tag/mammography-test/>.
- [15] "Concierge Radiologist," 23 02 2014. [Online]. Available: <http://www.conciergeradiologist.com/abnormal-mammogram.html>.
- [16] "Siemens Healthcare. Inspiration manual."
- [17] T. M. Adams and R. A. Layton, *Introductory MEMS, fabrication and applications*, New York: Springer, 2010.
- [18] "The Plastics Portal," [Online]. Available: <http://www.plasticseurope.org/what-is-plastic/types-of-plastics-11148/engineering-plastics/pmma.aspx>. [Accessed 31 03 2014].
- [19] B. W. Jensen, D. W. Breiby and K. West, "Base inhibited oxidative polymerization of 3,4-ethylenedioxythiophene with iron(III)tosylate," *Science Direct*, 2005.
- [20] A. Folch, *Introduction to BioMEMS*, CRC PRESS, 2013.
- [21] "Material property database," [Online]. Available: <http://www.mit.edu/~6.777/matprops/pdms.htm>. [Accessed 02 04 2014].
- [22] "Fujifilmusa," [Online]. Available: [https://www.fujifilmusa.com/shared/bin/Durimide%207500\\_US12.pdf](https://www.fujifilmusa.com/shared/bin/Durimide%207500_US12.pdf). [Accessed 31 03 2014].
- [23] "Elveflow," [Online]. Available: <http://www.elveflow.com/microfluidic-reviews-and-tutorials/pdms-membrane-thickness-of-a-spin-coated-pdms-layer>. [Accessed 24 03 2014].
- [24] T. S. Gates and M. A. Grayson, "On the use of accelerated aging methods for screening high temperature polymeric composite materials," *AIAA*, vol. 2, pp. 925-935, 1998.
- [25] "Arduino," [Online]. Available: <http://arduino.cc/>. [Accessed 07 05 2014].
- [26] "Matlab Central," [Online]. Available: <http://www.mathworks.com/matlabcentral/fileexchange/41602-i2c>

block-for-arduinoio-simulink-package. [Accessed 05 05 2014].

## 8 Appendix 2. Scientific article

### 8.1 Radiolucent pressure sensors - for mammography applications

Mammography is widely used today, where the purpose of the examination is to detect breast cancer. This is done by taking an x-ray image. To attain as good image quality as possible, the breast needs to be compressed, which is a very painful and uncomfortable experience for most women. Research has shown that the pressure is usually not evenly distributed and most of the pressure often ends up to close to the chest and a big amount over the pectoralis muscles. This causes unnecessary pain for most women and it can therefore be important to measure the specific pressure over more parts of the breast to possibly optimize applied pressure.

This project investigates the fabrication and design of a new type of pressure sensor that can be mounted directly on to the mammography machine. An important property of this sensor is that it is radiolucent, meaning it will not affect the resulting x-ray image taken of the patient's breast.

The sensor measures applied pressure and provides capacitance as an output. The benefits of this sensing mechanism is that it is not affected by temperature changes and works in small ranges. The capacitance is measured between two conducting layers, which are Poly(3,4-ethylenedioxythiophene) (PEDT), seen in figure 1. As pressure is applied on the sensor, the non-conducting materials compress and pull the PEDT layers closer to each other. This results in an increase in measured capacitance. By calibrating the capacitance to the applied pressure on the sensor it is possible to know what pressure is actually applied. In figure 1, the two PEDT layers actually consists of 3 "stripes" of PEDT. The result of this is that a matrix system containing 9 sensors.

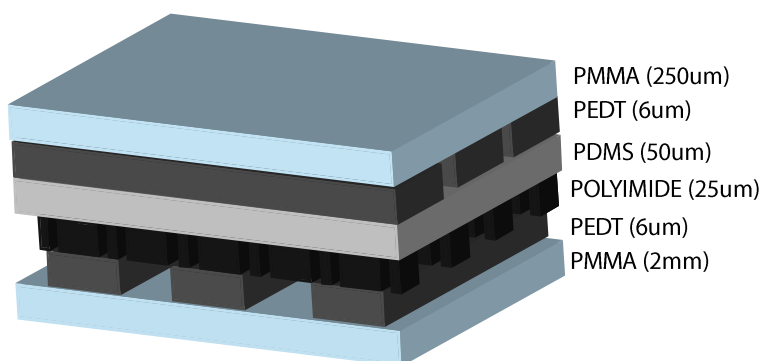


*Figure 1. Overview of the pressure sensor, the capacitance is measured between the two conducting PEDT layers.*

The fabrication of the pressure sensor was performed in clean-room facilities, and an overview of the sensor can be seen in figure 1. It consists of 6 layers, the three bottom layers and three upper layers were made separately and then put together. The lower and upper part consists of Polymethyl methacrylate (PMMA) which is a transparent and stiff plastic. The upper PMMA part is much thinner, for the reason to increase resolution. Resolution in this case refers to when pressure is applied at a point, it should not affect close individual sensors in the matrix.

PEDT is a polymer which is very robust and highly conductive. This polymer can be coated onto several materials and is the conducting material that the capacitance is measured between. Polydimethylsiloxane (PDMS) is a type of silicone rubber that has many applications. PDMS is very elastic and has unique flexibility properties. That characteristic is vital in the sensor since this is the material that deforms. Between the PDMS and the lower PEDT layer, a Polyimide layer is present and has been patterned, as seen in figure 1. This structure will take in the soft PDMS and make sure that it does not spread over the sensor. Thus, this design increase previously mentioned resolution.

The results showed that the pressure sensor was not visible in mammography screening, neither through image processing tools, nor by looking at it. In a mammography examination the pressure varies between 0-35kPa, and the sensor worked well in these ranges. It could be possible to use the pressure sensor in other applications as well. The output signal of the sensor might have to be changed (e.g. if the sensor needs to adapt to a measurement system), therefore more research is needed when it comes to what property the sensor will have when changing the thicknesses of the different layers.